

Supporting information.

Experimental Section

Materials

4,7,13,16,21,24-hexaoxa-1,10-diazabicyclo[8.8.8]hexacosane (cryptand[2,2,2], 98%) was purchased from TCI. $\text{Sc}_3\text{N}@I_h\text{-C}_{80}$ of 97% purity was purchased from SES Research. Sodium fluorenone ketyl ($\text{C}_{13}\text{H}_8\text{ONa}$) was obtained as described.¹ *o*-Dichlorobenzene ($\text{C}_6\text{H}_4\text{Cl}_2$) was distilled over CaH_2 under reduced pressure; *n*-hexane was distilled over Na/benzophenone. All operations on the synthesis of **1** and their storage were carried out in a MBraun 150B-G glove box with controlled atmosphere and water and oxygen content less than 1 ppm. The solvents were degassed and stored in the glove box. KBr pellets for IR- and UV-visible-NIR measurements were prepared in the glove box.

General

UV-visible-NIR spectra were measured in KBr pellets on a Perkin Elmer Lambda 1050 spectrometer in the 250-2500 nm range. FT-IR spectra ($400\text{-}7800\text{ cm}^{-1}$) were measured in KBr pellets with a Perkin-Elmer Spectrum 400 spectrometer or an AVATAR 360 FT-IR-spectrometer.

Synthesis

The crystals of $\{\text{cryptand}[2,2,2](\text{Na}^+)\}_2(\text{Sc}_3\text{N}@I_h\text{-C}_{80}^-)_2 \cdot 2.5\text{C}_6\text{H}_4\text{Cl}_2$ (**1**) were obtained by diffusion technique. 10 mg of $\text{Sc}_3\text{N}@I_h\text{-C}_{80}$ (0.009 mmol) was reduced by an excess of sodium fluorenone ketyl (3 mg, 0,0148 mmol) in the presence of equimolar amount of cryptand[2,2,2] (3.4 mg, 0.009 mmol) in 10 mL of *o*-dichlorobenzene during 6 hours at 100°C by intense stirring producing brown solution. It was cooled down to room temperature and filtered into the 50 mL glass tube of 1.8 cm diameter with a ground glass plug, and 30 mL of *n*-hexane was layered over the solution. The crystals were precipitated on the walls of the tube during 2 months. Then the solvent was decanted from the crystals and they were washed with *n*-hexane to yield black blocks up to $0.3 \times 0.2 \times 0.2\text{ mm}^3$ in size in 18% yield. Composition of the crystals was determined from X-ray diffraction analysis on single crystals. We tested several crystals from the synthesis and all of them show the same unit cell parameters. Therefore, they belonged to one crystal phase.

Calculations.

DFT computations of molecular structures and vibrational and excitation spectra of anionic dimes were performed using GGA PBE functional² and TZ2P-quality basis set implemented in Priroda package.^{3, 4} For MO visualization, single-point energy calculations at the PBE/TZVP level were performed using Orca suite.⁵ VMD code⁶ was used for visualization of molecules and isosurfaces.

X-ray crystal structure determination

Crystal data for **1**: C₂₁₁H₈₂Cl₅N₆Na₂O₁₂Sc₆, F.W. 3385.81, black prism, 0.220×0.110×0.006 mm³, 95(2) K. monoclinic, space group *P*2₁/*c*, *a* = 15.1344(9), *b* = 20.6079(13), *c* = 21.8351(12) Å, β = 90.019(6)°, *V* = 6810.1(7) Å³, *Z* = 2, *d*_{calcd} = 1.651 M gm⁻³, μ = 0.469 mm⁻¹, *F*(000) = 3438, 2θ_{max} = 48.262°; 50523 reflections collected, 10825 independent; *R*₁ = 0.1401 for 5385 observed data [*>* 2σ(*F*)] with 35972 restraints and 1935 parameters; *wR*₂ = 0.3943 (all data); final G.o.F. = 1.319. CCDC 1487746.

X-ray diffraction data for the crystal of **1** were collected on a Bruker Smart Apex II CCD diffractometer with graphite monochromated MoK_α radiation using a Japan Thermal Engineering Co. cooling system DX-CS190LD. Raw data reduction to *F*² was carried out using Bruker SAINT.⁷ The structure was solved by direct method and refined by the full-matrix least-squares method against *F*² using SHELX 2013.⁸ Non-hydrogen atoms were refined in the anisotropic approximation except for the disordered solvent molecules of 0.14-0.25 occupancies. Crystal sample was weak diffracting. High angle diffraction spots could not be detected, resulting in low data/parameters ratio.

Disorder in the crystal structure of **1**.

The (Sc₃N@I_h-C₈₀)₂ dimers are disordered in **1** between three orientations with the 0.441(3), 0.366(3) and 0.192(3) occupancies. Nevertheless, the geometry of the dimers and the Sc₃N fragments inside the cage as well as the presence of intercage C-C bonds between fullerenes in the dimers are well resolved. The cryptand[2,2,2](Na⁺) cations are statistically disordered between two equiprobable orientations approximately related by the mirror plane which transforms left-handed isomer of the cryptand into the right-handed one. There are two positions of solvent C₆H₄Cl₂ molecules in **1**. The solvent molecule at an inversion center is statistically disordered between four orientations with the 0.25 occupancies. The solvent molecule in a general position is disordered between four orientations with the 0.19/0.14/0.24/0.18 occupancies providing total 0.75 occupancy of the site. Due to strong disorder of all components great number of restraints was used for the crystal structure refinement. To keep fullerene geometry close to ideal one in the disordered groups, the bond length restraints were applied along with the next-neighbor distances, using the DFIX and SADI SHELXL instructions, respectively. To keep the anisotropic thermal parameters of the fullerene atoms within reasonable limits the displacement components were restrained using SIMU, ISOR and DELU SHELXL instructions. Thermal parameters of the cryptand atoms were also refined with the similar restraints. SAME SHELXL instructions were used to refine the Sc₃N orientations and the orientations of solvent molecules. Since the disorder gives a lot of additional refinement parameters, in order to reduce their amount the opposite atoms of the fullerene sphere were refined with equal thermal parameters using EADP SHELXL instructions; similar instructions was used for the atoms of two orientations of cryptand. Besides, non-hydrogen atoms of the

solvent molecules were treated isotropically and U_{iso} values for all carbon and all chlorine atoms were equated and refined as two free variables in the FVAR SHELXL instruction.

The structure of **1** can be solved in a monoclinic or an orthorhombic unit cell. Systematic absences correspond to *Pba2* or *Pbam* space group, however, the orthorhombic symmetry does not agree with the fullerene disorder. Electronic density on endometallofullerene is described well by three positions of the dimer in the monoclinic unit cell. At least four positions of the dimer should be used in the orthorhombic unit cell and even at such disorder pattern high residual electronic density is still observed and cannot be properly described. As a result, final *R*-factor in the monoclinic unit cell is lower than in the orthorhombic one. Therefore, we choose monoclinic *P2₁/c* space group for structure of **1**.

IR- spectra

Table S1. IR-spectra (cm⁻¹ in KBr) of starting compounds and salt **1**.

Components	Cryptand[2,2,2]	Sc ₃ N@I _h -C ₈₀	{cryptand[2,2,2](Na ⁺) ₂ (C ₆₀ ⁻) ₂ ·C ₆ H ₄ Cl ₂ ·C ₆ H ₁₄ ⁹	{cryptand[2,2,2](Na ⁺) ₂ (Sc ₃ N@I _h -C ₈₀ ⁻) ₂ ·2.5C ₆ H ₄ Cl ₂ (1)
Fullerene		Sc ₃ N@I _h -C ₈₀ 503w 600s 802w 1021m 1104m 1207m 1264w 1370s sh 1381s 1461m 1519w	C ₆₀ 514w 525w* 575s* 1183w 1393s	(Sc ₃ N@I _h -C ₈₀ ⁻) ₂ 500w 645m 658m 798m 802m 1030m* 1101vs* 1200w 1261m 1372s sh 1380s 1454s* 1519w
Cryptand	423w 476w 528w 581w 735m 922m 948w 982m 1038w 1071m 1100s 1127s 1213w 1295m 1329m 1360s 1446m 1462m 1490w 2790w 2877w 2943w		422w 466w 525w* 575s* 751m* 932m 943m - 1033w* - 1103s 1135m 1239w 1297m - 1353s - 1455m* 1478w 2813w 2881w 2957w	437w 467w 517w 560w 745m* 929m 941m - 1030m* 1077s 1101vs* 1134m 1200w 1300m - 1358s 1432m 1454s* 1480w 2807w 2868w 2961w
Solvent			658w 751m* 1033w* 1455m*	660w 745m* 1030m* 1454s*

* Bands are overlapped, w-weak intensity, m – middle intensity, s – strong intensity, sh – shoulder

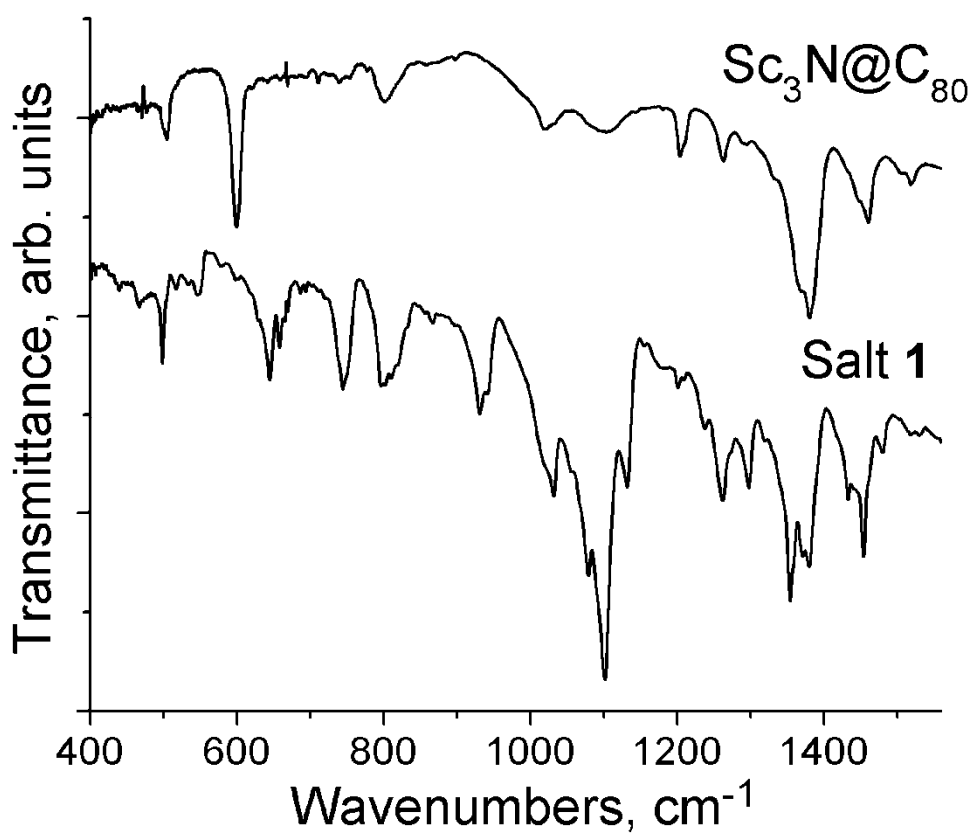


Figure S1. IR-spectra of starting $\text{Sc}_3\text{N}@I_h\text{-C}_{80}$ and salt $\{\text{cryptand}[2,2,2](\text{Na}^+)\}_2(\text{Sc}_3\text{N}@I_h\text{-C}_{80}^-)_2 \cdot 2.5\text{C}_6\text{H}_4\text{Cl}_2$ (**1**) in KBr pellets prepared in anaerobic conditions.

IR spectra of Sc₃N@C₈₀ and its dimer

The figure below shows experimental IR spectra of Sc₃N@I_h-C₈₀, its anionic dimer, as well as computed spectra of Sc₃N@C₈₀ and three isomers of the dimer (PHHJ, THJ, and “mixed”). Sc₃N@C₈₀ shows characteristic vibration of the Sc₃N cluster at 600 cm⁻¹. These twofold degenerate modes correspond to the in-plane motion of the nitride ion and can be described as antisymmetric Sc–N stretching mode $\nu_{\text{as}}(\text{Sc-N})$.^{10, 11} Theory gives reasonable agreement with the experimental spectrum except for the 500-600 cm⁻¹ range, where one mid-intensity predicted band has not observed in the experimental spectrum.

In the spectrum of the dimer, two characteristic bands can be pointed out. The $\nu_{\text{as}}(\text{Sc-N})$ mode is up-shifted and split into two main components at 645 and 658 cm⁻¹, respectively. According to the computations, dimerization results in lifting of the twofold degeneracy of the $\nu_{\text{as}}(\text{Sc-N})$ mode and the up-shift of its component with high IR intensity. Moreover, the frequency of the $\nu_{\text{as}}(\text{Sc-N})$ mode in the PHHJ and THJ dimers is somewhat different, which presumably gives complex shape of the experimental band. Vibration is visualized in Fig. S2. As can be seen, it can be described as a stretching vibration of the Sc-N bond aligned parallel to the intercage bond. Surprisingly, vibrations of other Sc-N bonds have much lower intensities and occur at lower frequencies (ca 540 cm⁻¹)

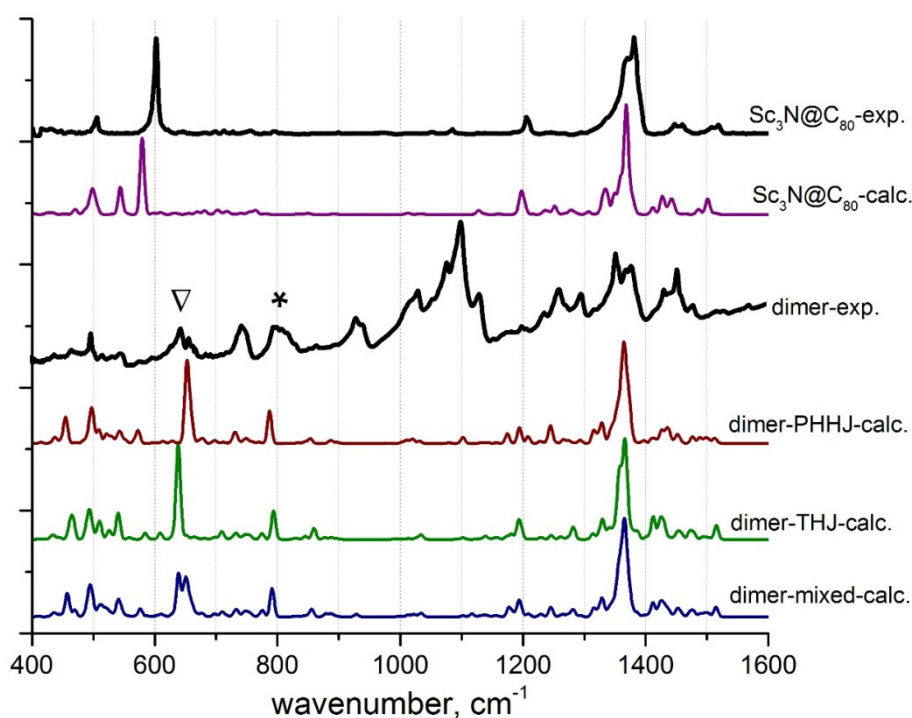


Figure S2. Experimental and computed IR spectra. Characteristic bands of the dimer discussed in the text are marked by a triangle and an asterisk.

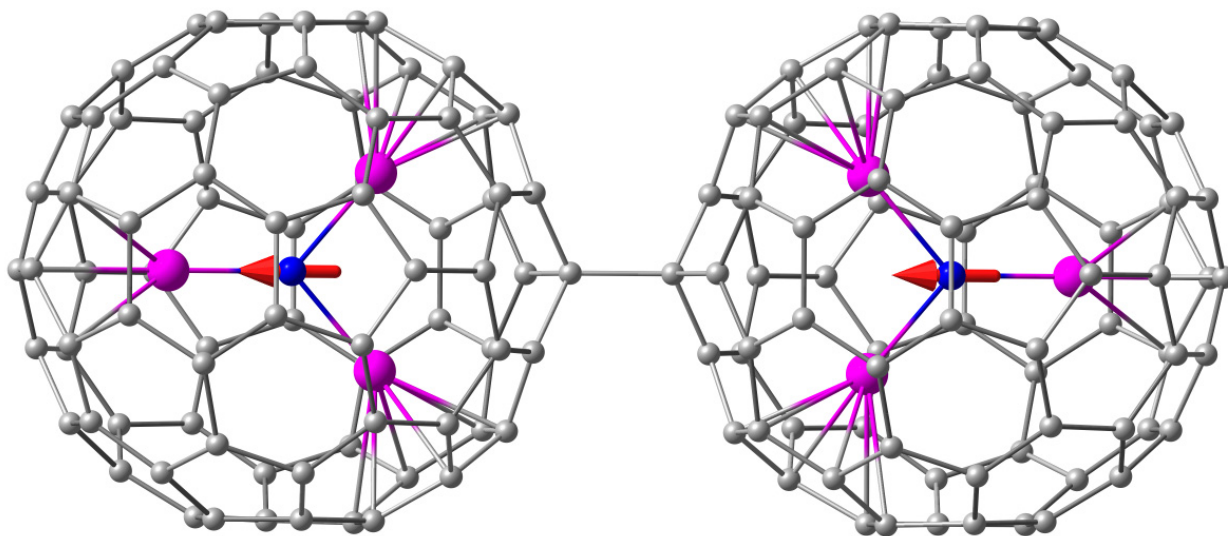


Figure S3. Vibrational displacement for the most intense component of the $\nu_{\text{as}}(\text{Sc-N})$ mode in the dimer (displacement is shown by red arrows)

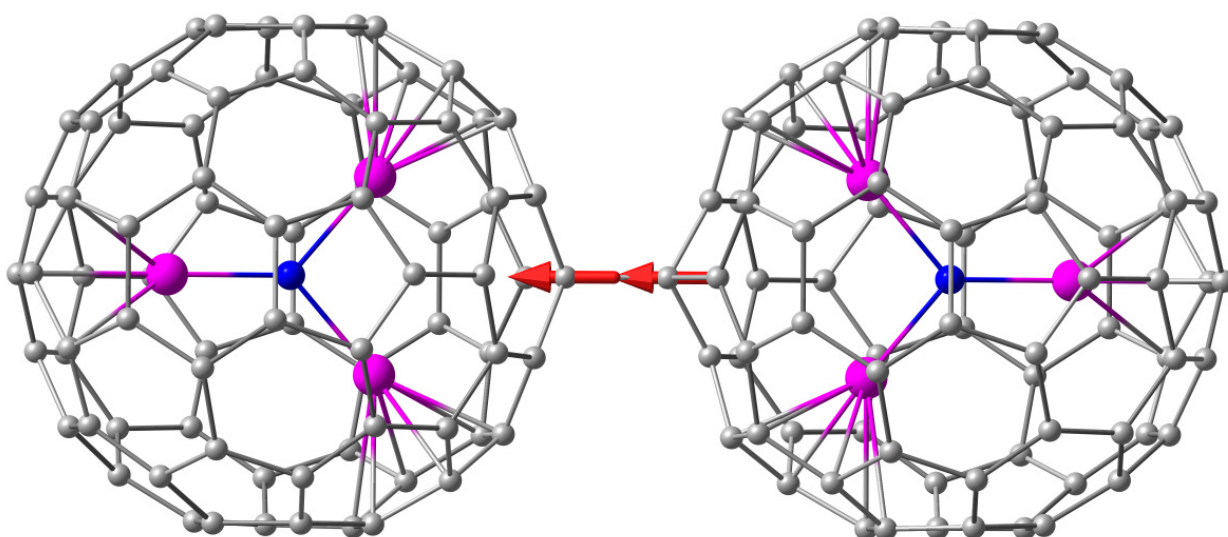


Figure S4. Vibrational displacement for the vibration of the intercage bond (displacement is shown by red arrows)

Another characteristic mode of the dimer is localized predominantly on the intercage bond and corresponds to the medium-intensity absorption bands near 798 and 802 cm^{-1} . Each anionic dimer has such a mode near $800\text{--}850\text{ cm}^{-1}$ as was discussed in detail in the paper on cationic $(\text{C}_{70}^+)_2$ dimer in $(\text{C}_{70}^+)_2(\text{Ti}_3\text{Cl}_{13}^-)_2$.¹²

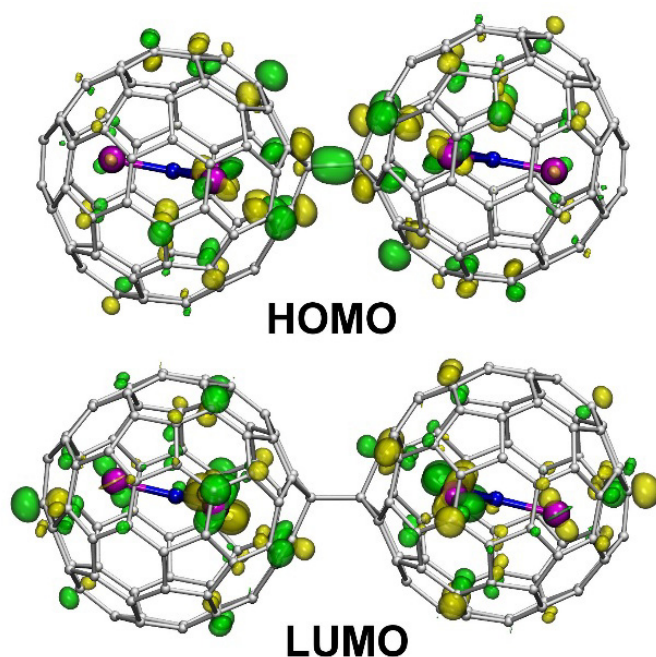


Figure S5. HOMO and LUMO of THJ dimers.

References

1. D. V. Konarev, S. S. Khasanov, E. I. Yudanov, R. N. Lyubovskaya, *Eur. J. Inorg. Chem.* **2011**, 816-820.
2. J. P. Perdew, K. Burke, M. Ernzerhof, *Phys. Rev. Lett.* **1996**, 77, 3865-3868.
3. D. N. Laikov, Y. A. Ustynuk, *Russ. Chem. Bull.* **2005**, 54, 820-826.
4. D. N. Laikov, *Chem. Phys. Lett.* **1997**, 281, 151-156.
5. F. Neese, *WIREs Comput. Mol. Sci.* **2012**, 2, 73-78.
6. W. Humphrey, A. Dalke, K. Schulten, *J. Molec. Graphics* **1996**, 14, 33-38.
7. Bruker Analytical X-ray Systems, Madison, Wisconsin, U.S.A, 1999.
8. G. M. Sheldrick, *Acta Cryst. Sec. A* **2008**, 64, 112.
9. D. V. Konarev, S. S. Khasanov, M. Ishikawa, E. I. Yudanov, A. F. Shevchun, M. S. Mikhailov, P. A. Stuzhin, A. Otsuka, H. Yamochi, G. Saito, R. N. Lyubovskaya, *Chem. Select*, **2016**, 1, 323-330.
10. M. Krause, H. Kuzmany, P. Georgi, L. Dunsch, K. Vietze, G. Seifert, *J. Chem. Phys.* 2001, 115, 6596-6605.
11. A. A. Popov, *J. Comput. Theor. Nanosci.* **2009**, 6, 292-317.
12. A. A. Popov, A. V. Burtsev, V. M. Senyavin, L. Dunsch, S. I. Troyanov, *J. Phys. Chem. A* **2008**, 113, 263-272.